# A point mutation in the murine *Hem1* gene reveals an essential role for Hematopoietic Protein 1 in lymphopoiesis and innate immunity

Heon Park,[1] Karen Staehling-Hampton,[2] Mark W. Appleby,[2] Mary E. Brunkow,[2] Tania Habib,[1] Yi Zhang,[2] Fred Ramsdell,[2] H. Denny Liggitt,[1] Brian Freie,[3] Mark Tsang,[1] George Carlson,[4] Sherree Friend,[5] Charles Frevert,[1] and Brian M. Iritani[1,3]

[1]The Department of Comparative Medicine, University of Washington, Seattle, WA 98195
[2]Celltech R & D, Inc., Bothell, WA 98021
[3]Division of Basic Sciences, Fred Hutchinson Cancer Research Center, Seattle, WA 98109
[4]The McLaughlin Research Institute, Great Falls, MT 59405
[5]Amnis, Inc., Seattle, WA 98121

**Hem1 (Hematopoietic protein 1) is a hematopoietic cell-specific member of the Hem family of cytoplasmic adaptor proteins. Orthologues of Hem1 in *Dictyostelium discoideum*, *Drosophila melanogaster*, and *Caenorhabditis elegans* are essential for cytoskeletal reorganization, embryonic cell migration, and morphogenesis. However, the in vivo functions of mammalian Hem1 are not known. Using a chemical mutagenesis strategy in mice to identify novel genes involved in immune cell functions, we positionally cloned a nonsense mutation in the *Hem1* gene. Hem1 deficiency results in defective F-actin polymerization and actin capping in lymphocytes and neutrophils caused by loss of the Rac-controlled actin-regulatory WAVE protein complex. T cell development is disrupted in Hem1-deficient mice at the $CD4^{-}CD8^{-}$ (double negative) to $CD4^{+}CD8^{+}$ (double positive) cell stages, whereas T cell activation and adhesion are impaired. Hem1-deficient neutrophils fail to migrate in response to chemotactic agents and are deficient in their ability to phagocytose bacteria. Remarkably, some Rac-dependent functions, such as Th1 differentiation and nuclear factor κB (NF-κB)–dependent transcription of proinflammatory cytokines proceed normally in Hem1-deficient mice, whereas the production of Th17 cells are enhanced. These results demonstrate that Hem1 is essential for hematopoietic cell development, function, and homeostasis by controlling a distinct pathway leading to cytoskeletal reorganization, whereas NF-κB–dependent transcription proceeds independently of Hem1 and F-actin polymerization.**

CORRESPONDENCE
Brian M. Iritani:
biritani@u.washington.edu

Abbreviations used: CBC, complete blood count; DN, double negative; DP, double positive; ENU, N-ethylnitrosourea; Erk, extracellular regulated mitogen-activated protein kinase; GTP, guanosine-5′-triphosphate; HSC, hematopoietic stem cell; siRNA, small inhibitory RNA; SP, side population; WBC, white blood cell.

Reorganization of the actin cytoskeleton is essential for many active cellular functions in immune cells including cell migration, adhesion, phagocytosis, transcription, and cytokinesis (for review see reference 1). Among the major signaling molecules that regulate the cytoskeleton include members of the Rho family of guanosine triphosphatases (Cdc42, Rho, and Rac). Rho family members are activated downstream of multiple receptor types, including BCR and TCR, growth factor receptors, and cytokine receptors, and are also known to activate integrin receptors and cell adhesion through "inside-out" signaling (2). The importance of Rac in hematopoietic cell development and function is underscored by the characterization of gene-targeted mutations in mice,

M.W. Appleby and F. Ramsdell's present address is ZymoGenetics, Inc., Seattle, WA 98102.

K. Staehling-Hampton's present address is Stowers Institute for Medical Research, Kansas City, MO 64110.

Y. Zhang's present address is Amgen Inc, San Francisco, CA 94080.

The online version of this article contains supplemental material.

© 2008 Park et al. This article is distributed under the terms of an Attribution–Noncommercial–Share Alike–No Mirror Sites license for the first six months after the publication date (see http://www.jem.org/misc/terms.shtml). After six months it is available under a Creative Commons License (Attribution–Noncommercial–Share Alike 3.0 Unported license, as described at http://creativecommons.org/licenses/by-nc-sa/3.0/).

The Rockefeller University Press $30.00
J. Exp. Med. Vol. 205 No. 12 2899-2913
www.jem.org/cgi/doi/10.1084/jem.20080340



The Journal of Experimental Medicine

as well as natural mutations in humans, which result in a plethora of alterations including impaired proliferation, IL-2 production, adhesion, and migration in T cells (3, 4); defective dendrite formation and antigen presentation by DCs (5); defective migration (6), adhesion (7), and phagocytosis (8) by neutrophils; and impaired proliferation, survival, adhesion, and homing of hematopoietic stem cells (HSCs) (9–13). Rac and Rho are essential for pre–T cell receptor-mediated T cell development (14–16), whereas Rac is also essential for B cell development and survival (17). These studies indicate that Rho family members are essential for several active biological processes in hematopoietic cells.

Remarkably, although there are 70 or more putative Rho family effector proteins (18), there is limited information on the identity of their biologically important targets in hematopoietic cells. Genetic studies in *Drosophila melanogaster* and *Caenorhabditis elegans* suggest that key biological targets of Rho family members may involve a family of adaptor proteins, including WASp (Wiskott-Aldrich Syndrome protein), and components of the WAVE complex. In mammalian cells, the WAVE complex consists of multiple subunits including WAVE (1, 2, or 3), HSPC300, Abi (1 or 2), Hem2 (also known as Nap1 [Nck-associated protein 1]), and Sra1 (see Fig. 8) (19). The WAVE complex induces actin polymerization in response to Rac guanosine-5′-triphosphate (GTP), which is brought into the WAVE complex via associations with Sra1 and Hem2. Although the majority of WAVE complex subunits are ubiquitously expressed, there is a version of the Hem subunit called Hem1 (also known as Nckap1l [NCK-associated protein1-like]), which was cloned based on hybridization to transcripts from hematopoietic cells (20). Biochemical and genetic studies in *D. melanogaster* (21), *C. elegans* (22), *Arabidopsis thaliana* (23), and *Dictyostelium discoideum* (24) indicate that homologues of Nap1 act downstream of the Rac pathway to regulate the actin polymerization, cell migration, and cell shape that are necessary for proper morphogenesis and development.

In this study, we sought to identify novel genes involved in lymphocyte development by taking a "phenotype-driven" approach using N-ethylnitrosourea (ENU) mutagenesis, followed by immune function screening of G3 animals for recessive mutations leading to specific immunodeficiencies. Using positional cloning strategies, we identified a pedigree of mice that contains a point mutation in the *Hem1* gene, resulting in the absence of Hem1 protein. We show that Hem1 is an essential hematopoietic-specific regulator of the actin cytoskeleton, where it controls lymphocyte development, activation, proliferation, and homeostasis, as well as phagocytosis and migration by neutrophils and macrophages. Surprisingly, cytokine production proceeds normally in the absence of Hem1, suggesting that NF-κB–dependent transcription of proinflammatory cytokines is regulated independently of Hem1 and the actin cytoskeleton.

## RESULTS

### Generation of *Hem1*–deficient mice using chemical mutagenesis

In the course of the ENU program, a flow cytometry screen identified a pedigree (denoted NTB.1 for no T or B cells) in which the mice presented with an increased percentage of $CD11b^+$ myeloid cells and a decreased percentage of $B220^+$ B lymphocytes in peripheral blood samples (Fig. 1 A). To identify the gene responsible for the NTB.1 phenotype, G1 and G2 NTB.1 carriers were crossed to C3HeB/FeJ mice, and the resulting F1 animals were intercrossed to generate F2 and N2 animals for mapping (see Materials and methods). The levels of $B220^+$ B cells in peripheral blood were assessed in the resultant generations. A genome scan of affected and unaffected animals indicated that the NTB.1 mutation mapped to chromosome 15 between 59.8 and 60.1 cM. Candidate genes were sequenced and a single-nucleotide polymorphism was identified in exon 13 of the *Hem1* gene, which changed a CAG (Gln) to TAG (stop), resulting in premature termination at residue 445 (Fig. 1 B). Immunoblotting of whole cell lysates from normal littermate and *Hem1* mutant thymocytes, splenocytes, and BM cells with an anti-Hem1 antibody (25) revealed the absence of Hem1 protein in mice homozygous for the NTB.1 mutation (Fig. 1 C; and see Fig. 7 F).

### *Hem1* is expressed predominantly in hematopoietic cells

A previous Northern blot study using cell lines derived from various tissues suggested that *Hem1* expression is restricted to hematopoietic tissues (20). We performed a more extensive survey of *Hem1* expression using real-time PCR for *Hem1* message in cDNA derived from 25 different mouse tissues. We find that although *Hem-* is predominantly expressed in hematopoietic tissues, it is also expressed in urogenital tissues including testis (Fig. S1, available at http://www.jem.org/cgi/content/full/jem.20080340/DC1). In contrast, *Hem2* is not expressed in hematopoietic tissues but is widely expressed in many other tissues (Fig. S1). Indeed, mice deficient in *Hem2* die around embryonic day 8.5–10.5 because of morphological abnormalities ranging from severe neurulation defects to complete resorption (26).

We next characterized the expression pattern of *Hem1* in different hematopoietic cell lineages and progenitor cells. We find that *Hem1* is expressed in lineage-negative ($Lin^-$) $Sca1^+$ $cKit^+$ side population $(SP)^+$ cells, which are highly enriched for HSCs, as well as $Lin^-Sca1^+cKit^+$ $SP^-$ cells and $Lin^-Sca1^-cKit^-$ cells, which contain early progenitors (Fig. S1). *Hem1* is also expressed in B and T cell progenitors during all stages of maturation and in purified macrophages and neutrophils (Fig. S1). The results collectively indicate that *Hem1* is predominantly expressed in developing and mature hematopoietic cells, whereas *Hem2* is expressed in nonhematopoietic cells.

### Hem1-deficient mice exhibit lymphopenia, neutrophilia, and anemia

We performed complete blood counts (CBCs) and differential cell counts to determine the representation of mature hematopoietic cell types in peripheral blood from $Hem1^{-/-}$ and normal WT littermate mice. We find that loss of Hem1 results in a moderate increase in total white blood cells (WBCs) per microliter of blood, which corresponds to a 25-fold increase in the number of neutrophils and a 3.5-fold decrease

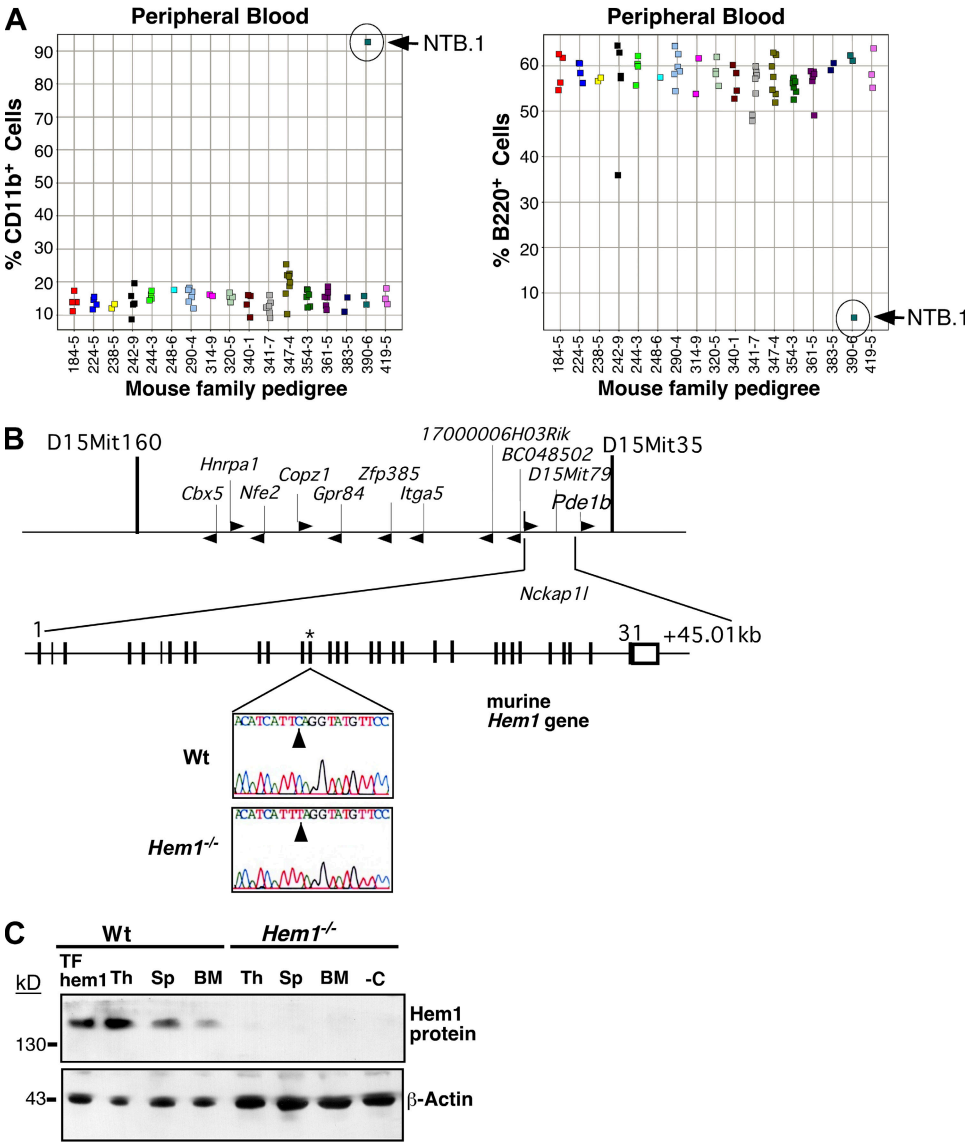


**Figure 1. Generation and identification of *Hem1* mutant mice by ENU mutagenesis.** (A) Recessive mutant (NTB.1) obtained from a G3 pedigree was found to display a high percentage of CD11b+ and a low percentage of B220+ cells in peripheral blood. Blood cells were stained with fluorescent α-CD11b and α-B220 followed by flow cytometry. The percentage of CD11b- and B220-positive cells in blood is shown, where each symbol represents an individual mouse and each color (column) represents a unique G3 family pedigree, which is denoted by numbers on the x axis. (B) Genomic structure of the mouse *Hem1* gene. The location of a C–T conversion induced by ENU mutagenesis in the 13th exon of the *Hem1* gene is shown. (C) A representative immunoblot of two experiments showing the absence of Hem1 protein in hematopoietic tissues of $Hem1^{-/-}$ mice compared with normal littermates. Whole cell lysates were generated from thymocytes (Th), splenocytes (Sp), and BM cells. TFhem1, positive control from *pCDNA3.1-Hem1*–transfected 293T cells; −C, negative control from empty *pcDNA3.1*–transfected 293T cells.

in the number of lymphocytes per microliter of blood in $Hem1^{-/-}$ mice compared with WT mice (Figs. 2, A–C). $Hem1^{-/-}$ mice also exhibit altered RBC indices, such as decreased hematocrit and mean corpuscular volume (MCV; Fig. 2 A), with reticulocytosis (increased RBC progenitors; Fig. 2 D), anisocytosis (variation in RBC size), echinocytosis (membrane spickles), and poikilocytosis (abnormally shaped RBC), which is characterized by keratocytes (horned-shaped cells), dacryocytes (tear-shaped cells), schistocytes (RBC fragmentation), and acanthocytes (thorny cells; Fig. 2 E and not depicted). $Hem1^{-/-}$ RBCs exhibit increased fragility relative to WT RBCs, as measured by an increased percentage of lysis in response to hypotonic NaCl solutions (Fig. 2 F). Collectively, these RBC indices are suggestive of a microcytic hypochromic hemolytic anemia in $Hem1^{-/-}$ mice, which parallels the anemia phenotype of Rac-deficient mice (27).

Gross and histological examination of $Hem1^{-/-}$ mice reveal a spectrum of lesions, including dense amyloid accumulations containing foci of mineral at the margins of the liver (Fig. 2 G), and occasional diffuse inflammation in the liver,

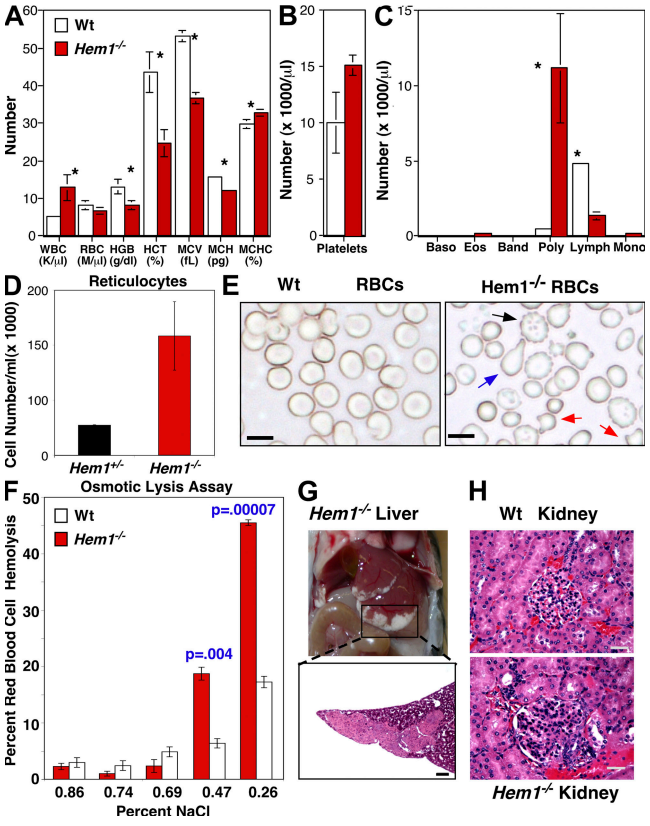


**Figure 2. Loss of Hem1 results in lymphopenia, neutrophilia, and induces tissue-specific pathology.** (A–C) CBCs and differential cell counts were performed on peripheral blood from *Hem1*$^{-/-}$ and normal littermate control mice (WT). Shown are the mean ± SEM from four mice/group. WBC, total WBC; RBC, total RBC; HGB, hemoglobin; HCT, hematocrit; MCV, mean corpuscular volume; MCH, mean corpuscular hemoglobin, MCHC, mean corpuscular hemoglobin concentration; Baso, basophils; Eos, eosinophils; Poly, neutrophils; Lymph, lymphocytes; Mono, monocytes. An asterisk denotes significant differences between mutant and WT littermates. WBC, P = 0.06; hemoglobin, P = 0.05; hematocrit, P = 0.02; mean corpuscular volume, P = 0.00005; mean corpuscular hemoglobin, P = 0.004; mean corpuscular hemoglobin concentration, P = 0.05; neutrophils, P = 0.03; lymphocytes, P = 0.00006. (D) *Hem1*$^{-/-}$ mice exhibit increased immature erythrocytes (reticulocytes) in blood. The number of reticulocytes per microliter of blood are represented (mean ± SEM for four animals per group). (E) Representative blood smears of four mice/group of erythrocytes from WT and *Hem1*$^{-/-}$ mice were imaged under 400× magnification. *Hem1*$^{-/-}$ erythrocytes show morphological abnormalities such as anisocytosis (variation in size), echinocytes or schistocytes (black arrow), keratocytes (red arrows), and dacryocytes (blue arrow). Bars, 5 μm. (F) *Hem1*$^{-/-}$ erythrocytes exhibit increased fragility. RBCs from WT or *Hem1*$^{-/-}$ mice were added to decreasing (hypotonic) solutions of NaCl. After centrifugation, the OD of the supernatant at 540 nm was assessed to determine the amount of hemoglobin released into the supernatant. Shown is a bar graph depicting the mean ± SEM of the percent lysis of WT ($n$ = 5) and *Hem1*$^{-/-}$ ($n$ = 5) RBCs. (G and H) Hematoxylin and eosin staining was performed in tissue sections from liver and kidney. Images are representative of six mice/group. (G) At necropsy, *Hem1*$^{-/-}$ mice commonly exhibit whitish liver margins that are histologically represented as dense accumulations of amyloid interspersed with mineral and fibrous tissue. 10× power; bar, 100 μm. (H) Renal glomeruli from *Hem1*$^{-/-}$ mice frequently have an increase in mesangial matrix and cellularity consistent with membranoproliferative glomerulopathy. 40× power; bars, 50 μm.

epididymis, mesentery, thoracic pleura, heart, and lungs (not depicted). Membranoproliferative glomerulopathy (Fig. 2 H) and diffuse lymphoid hypoplasia are also common lesions, whereas myocardial fibrosis, amyloidosis, and pancreatic atrophy occur less frequently (not depicted). *Hem1*$^{-/-}$ spleens are substantially enlarged, even though lymphoid cells are depleted, because of marked proliferation of myeloid and erythroid progenitors (Fig. S2, available at http://www.jem.org/cgi/content/full/jem.20080340/DC1), which is indicative of extramedullary hematopoiesis. *Hem1*$^{-/-}$ thymi are hypoplastic, and lack the normal cortical/medullary architecture evident in WT thymi (unpublished data).

We next examined the potential of clonogenic hematopoietic progenitor cells in the BM, spleen, and blood from *Hem1*$^{-/-}$ and WT mice. We performed in vitro quantitation of myeloid (CFU-GM), erythroid (burst forming units-erythroid [BFU-E]), and multi-lineage (CFU-granulocyte/erythroid/macrophage/monocyte [CFU-GEMM]) assays using standard techniques. We find a significant reduction in CFU-GM, BFU-E, and CFU-GEMM in BM from *Hem1*$^{-/-}$ mice compared with WT BM (Fig. S2). In contrast, there is a dramatic increase in CFU-GM, BFU-E, CFU-GEMM colonies in spleens and peripheral blood from *Hem1*$^{-/-}$ mice compared with WT mice. This correlates with a fourfold increase in the percentage of Lin$^{-}$Sca1$^{+}$cKit$^{-}$ cells in the spleens of *Hem1*$^{-/-}$ mice compared with WT mice, which is consistent with increased mobilization of HSC and progenitors (HSC/Ps) from the BM to peripheral blood and spleen (Fig. S2).

### Hem1 is required for migration, phagocytosis, and F-actin polymerization in neutrophils

*Hem1*$^{-/-}$ mice exhibit an increase in the percentage (Fig. 3, A and B) and total number (not depicted) of cells bearing Mac1 and Gr1 (Fig. 3, A and B [top]), and CD61 (Fig. 3, A and B [bottom]) in the BM and spleen relative to WT mice, suggesting that myeloid cell homeostasis is altered by loss of Hem1 protein. We next determined whether loss of Hem1 affects neutrophil and macrophage functions. Purified neutrophils from *Hem1*$^{-/-}$ and WT mice were loaded into trans-well plates, and the ability of cells to migrate through a filter containing different concentrations of MLP (a tripeptide chemoattractant) was measured. *Hem1*$^{-/-}$ neutrophils fail to migrate efficiently across the filter in response to different concentrations of fMLP (Fig. 3 C). *Hem1*$^{-/-}$ neutrophils are also deficient in their ability to phagocytose fluorescent-conjugated beads (Fig. 3 D) and bacteria (not depicted) in response to MLP stimulation, as measured by flow cytometry. Likewise, *Hem1*$^{-/-}$ macrophages are deficient in their ability to phagocytose fluorescent-labeled *Escherichia coli* after 2 and 4 h of stimulation, relative to WT macrophages (Fig. 3 E). However, *Hem1*$^{-/-}$ macrophages produce normal or increased levels of the cytokines IL1β, TNF-α, Mip2 (macrophage-inflammatory protein 2), and cytokine-induced neutrophil chemoattractant (KC) after stimulation with *E. coli* or LPS, and the transcription of the corresponding genes, as well as *IL-23*, are increased (Fig. S3, available at http://www.jem.org/cgi/content/full/jem.20080340/DC1).

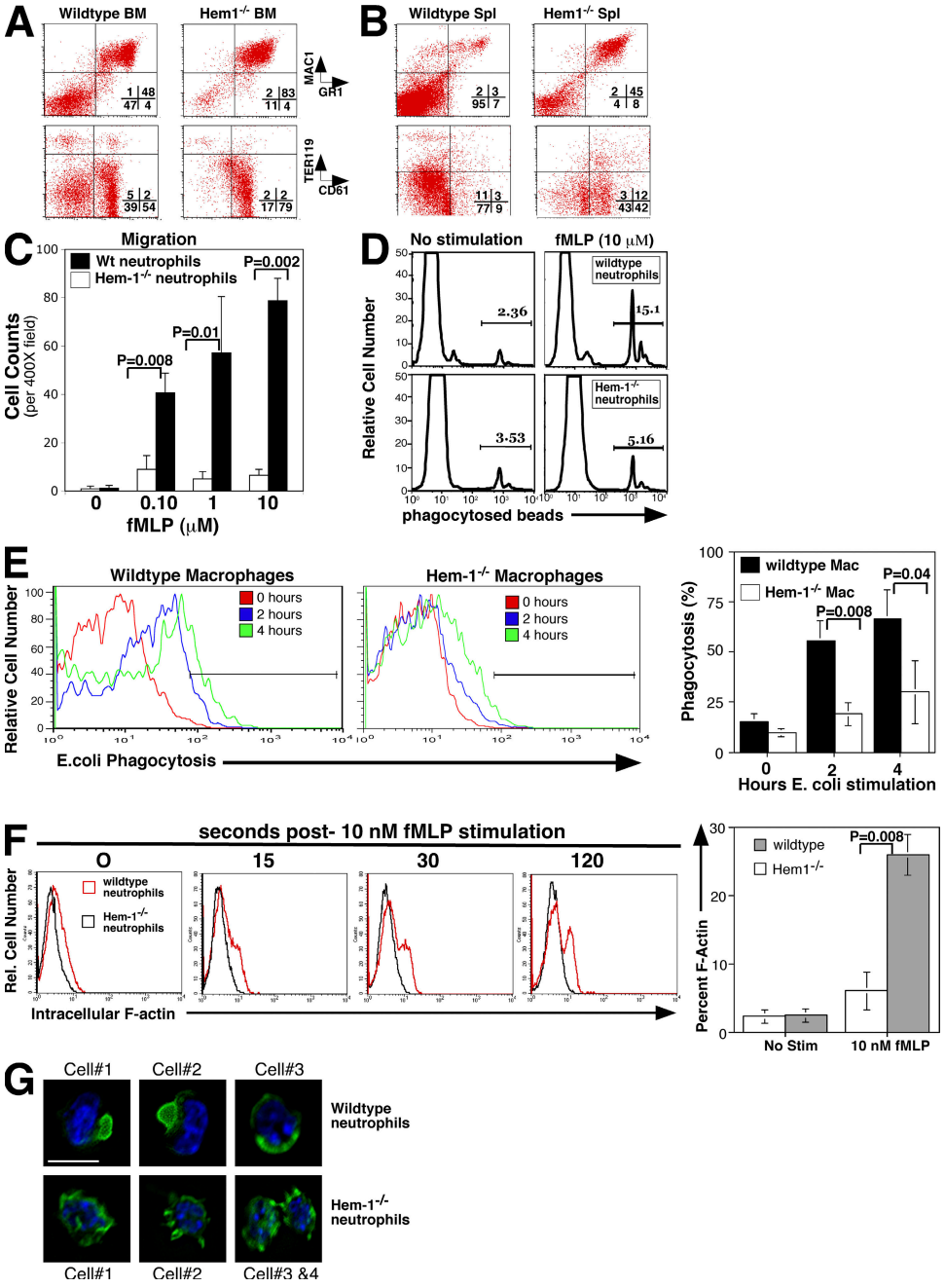


**Figure 3. Hem1–deficient neutrophils exhibit defective migration, phagocytosis, and F-actin polymerization.** (A and B) Total BM and splenocytes were stained with fluorescent-conjugated α-MAC1 and α-GR1 or α-Ter119 and α-CD61 antibodies followed by flow cytometry. The percentage of monocyte (Mac1$^+$), granulocyte (GR1$^+$), erythroid precursor (Ter119$^+$), and megakaryocyte (CD61$^+$) populations are shown in the representative histogram of eight mice per group. (C) BM-derived neutrophils were stimulated for 45 min with different concentrations of MLP to determine chemotactic ability across a membrane. The number of migrated cells (at 400×) was counted for three random fields and the mean ± SEM values are displayed on y axis. P-values are shown. Data are representative of three independent experiments. (D) $10^5$ neutrophils from WT and *Hem1*$^{-/-}$ BM were cultured with fluorescent 1-µm diameter microspheres for 5 min. Phagocytosis was measured by flow cytometry. The single-parameter histograms are representative of four experiments. (E) Peritoneal macrophages were incubated with fluorescent-conjugated *E. coli* for 0, 2, and 4 h. Phagocytosis was measured by flow cytometry. Bars represent the mean ± SEM from three independent experiments. P-values are shown. (F) BM-derived neutrophils were stimulated with 10 nM MLP. F-actin polymerization was determined at the time points indicated by flow cytometry after intracellular Alexa Fluor 488 phalloidin staining. The mean ± SEM of three animals per group (120-s time point) are shown in the bar graph. (G) BM-derived neutrophils from WT and *Hem1*$^{-/-}$ mice were stimulated with FMLP for 15 s. F-actin polymerization and capping formation were determined by confocal microscopy using Alexa Fluor 488 phalloidin (green) and DAPI (blue) staining. Bar, ∼12–15 µm.

The polymerization of F-actin is critical for forming phagosomes, as well as lamellipodia and filopodia, which are fingerlike projections responsible for polarizing the cytoskeletal machinery during cell migration. As shown in Fig. 3 F, >25% of WT neutrophils polymerize F-actin after 15 s of MLP treatment, as determined by increased phalloidin staining, whereas <5% of *Hem1*$^{-/-}$ cells polymerize F-actin even after 120 s of MLP stimulation. Deconvolution images reveal that polymerized F-actin in *Hem1*$^{-/-}$ cells is distributed diffusely in the cytoplasm, whereas F-actin in WT cells is clearly polarized toward the leading edge (Fig. 3 G). Transfection of *Hem1* cDNA into BM-derived neutrophils (28) from WT or *Hem1*$^{-/-}$ mice resulted in restoration of F-actin polymerization in response to MLP stimulation (Fig. S4, available at http://www.jem.org/cgi/content/full/jem.20080340/DC1). The results collectively indicate that Hem1 is required in innate immune cells for a variety of functions dependent on F-actin polymerization and cytoskeletal reorganization, including phagocytosis and migration.

### Lymphocyte development is impaired in Hem1-deficient mice

Because *Hem1*-deficient mice are lymphopenic, we examined whether T and/or B cell development are impaired. The development of lymphocytes can be broken down into many distinct stages based on the presence or absence of particular intracellular and surface proteins, as determined by flow cytometry (29, 30). As shown in Fig. 4 A, *Hem1*$^{-/-}$ mice have a 30-fold mean reduction in thymocyte number with an impairment in αβ T cell development within the CD4$^-$CD8$^-$ double-negative (DN) to CD4$^+$CD8$^+$ double-positive (DP) cell transition at the CD25$^{mid}$CD44$^-$ (DN3) to CD25$^-$CD44$^-$(DN4) cell stage, which is mediated by formation of the preTCR. The number of γδ thymocytes is also decreased, albeit to a lesser extent than αβ T cells (Fig. 4, A and B). The total numbers of peripheral CD4, CD8, and γδ T cells (Fig. 4 B) and B lymphocytes (not depicted) are reduced by at least 75%. The ratio of Foxp3$^+$CD4$^+$ T regulatory cells ($T_{reg}$) to Foxp3$^-$CD4$^+$ T cells is significantly higher in both thymus (Fig. 4 A) and spleen (Fig. 4 B), suggesting that Hem1 regulates both lymphocyte development and homeostasis.

### *Hem1*$^{-/-}$ hematopoietic stem and progenitor cells compete poorly with WT cells in BM chimeras

To determine if the defects in T and B cell development are autonomous to hematopoietic cells or are caused by a defective microenvironment, we transferred marked Lin$^-$ (lineage negative; Fig. 5) or total BM cells (Fig. S5, available at http://www.jem.org/cgi/content/full/jem.20080340/DC1) from WT (CD45.1$^+$ marker), *Hem1*$^{-/-}$ (CD45.2$^+$), or mixed WT and *Hem1*$^{-/-}$ Lin$^-$ cells into unirradiated (Fig. 5), or lethally irradiated (Fig. S5), *Rag2*$^{-/-}\gamma c^{-/-}$ (recombinase activating gene 2/common γ chain double-null) hosts (CD45.2$^+$), and lymphocyte development was analyzed 8–20 wk after transplant. As shown in Fig. 5 A, *Rag2*$^{-/-}\gamma c^{-/-}$ mice are completely blocked in T cell development at the CD4$^-$CD8$^-$ DN stage (columns 1 and 2). Injection of WT Lin$^-$ cells into *Rag2*$^{-/-}\gamma c^{-/-}$ mice completely reconstitutes T cell development in the thymus,

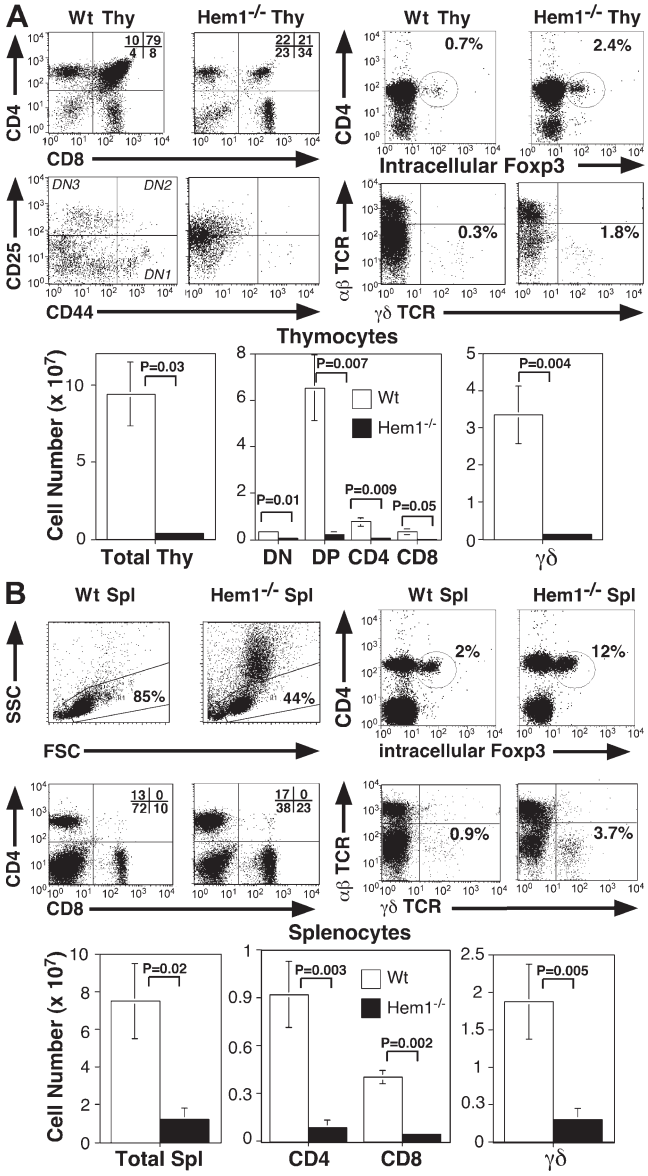


**Figure 4. T cell development is severely impaired in Hem1-deficient mice.** Total thymocytes (A) and splenocytes (B) from *Hem1*$^{-/-}$ and WT littermate mice were stained with fluorescent-conjugated α-CD4, α-CD8, α-CD3ε, α-CD25, α-CD44, α-B220, α-GR1, α-TCR-γδ, α-TCR-β, and intracellular α-Foxp3 and analyzed by flow cytometry. Representative histograms of eight mice per group of cells that fall within a forward scatter (FSC) and side scatter (SSC) lymphocyte gate are shown. Total thymocyte and splenocyte number were multiplied by the percentage of cells that fell within each quadrant to obtain the total number of cells within each developmental subset (right). Cells negative for B220, GR1, CD4, and CD8 were analyzed with CD44 and CD25 staining to determine the DN1-DN4 fractions. Bars represent the mean ± SEM from eight mice. P-values are shown. The high side scatter cells in *Hem1*$^{-/-}$ spleens are myeloid and progenitors cells.

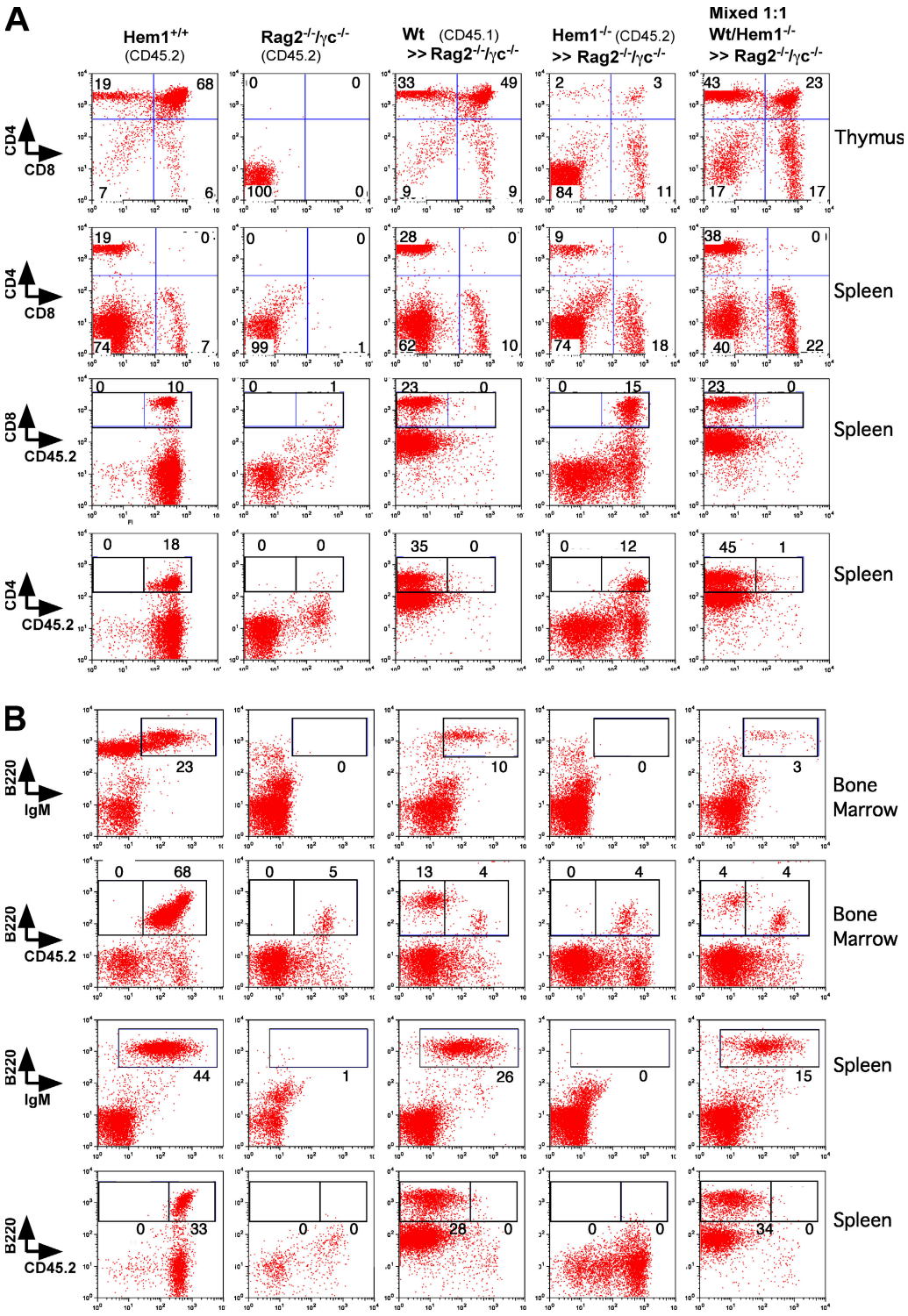


**Figure 5. Impaired T and B cell development in *Hem1* mutant mice is cell autonomous.** Lin$^-$ cells from *Hem1*$^{-/-}$ (CD45.2), WT (CD45.1), or mixed WT/*Hem1*$^{-/-}$ (1:1) were injected i.v. into *Rag2*$^{-/-}\gamma c^{-/-}$ recipient mice. Thymocytes, BM, and splenocytes were harvested from the recipient mice 8–15 wk after transplantation and analyzed by flow cytometry using fluorescent-conjugated α-CD4, α-CD8, α-CD45.1, α-B220, α-IgM, α-CD45.2, and α–TCR-β. (A) Representative dot-plot histograms of three independent experiments showing CD4, CD8, and TCR-β expression in conjunction with CD45.2 markers on thymocytes and splenocytes from the indicated chimeric mice. (B) Representative dot-plot histograms showing B220 and IgM, in conjunction with CD45.2 markers on BM and spleen cells from the indicated chimeric mice.

leading to normal representation of CD4 and CD8 cells in the spleen (Fig. 5 A, column 3). In contrast, *Hem1*$^{-/-}$ Lin$^-$ cells poorly reconstitute the thymi of *Rag2*$^{-/-}\gamma c^{-/-}$ mice, with the majority of cells residing at the DN stage (Fig. 5 A, column 4). *Hem1*$^{-/-}$ CD4 and CD8 SP cells can mature and expand in *Rag2*$^{-/-}\gamma c^{-/-}$ hosts, as determined by the presence of CD4$^+$CD45.2$^+$ and CD8$^+$CD45.2$^+$ cells in the spleen of transplanted mice. However, when *Hem1*$^{-/-}$ Lin$^-$ cells are mixed with WT Lin$^-$ cells at 1:1, 10:1, or 20:1 (*Hem1*$^{-/-}$/WT) ratios, they fail to reconstitute the thymus or spleen of transplanted mice, as determined by the presence of CD4 and CD8 cells bearing the CD45.1 (WT) but not CD45.2 markers (Fig. 5 A column 5; Fig. S5; and not depicted). The inability of *Hem1*$^{-/-}$ hematopoietic cells to compete with WT hematopoietic cells in BM chimeras is not caused by inadequate space in the BM niche because we obtain similar results after transplantation of WT, *Hem1*$^{-/-}$, or mixed 1:10 WT:*Hem1*$^{-/-}$ Lin$^-$ or total BM cells into lethally irradiated *Rag2*$^{-/-}\gamma c^{-/-}$ hosts (Fig. S5 and not depicted). *Hem1*$^{-/-}$ BM cells can contribute to the generation of GR-1$^+$ myeloid cells when mixed 1:10 WT/*Hem1*$^{-/-}$ BM cells and transplanted into lethally irradiated *Rag2*$^{-/-}\gamma c^{-/-}$ hosts, indicating that HSC/Ps are able to home to the BM niche in mixed BM chimeras (Fig. S5). In addition, *Hem1* heterozygous (+/−) BM cells compete normally with WT BM cells to produce CD4$^+$, CD8$^+$, GR1$^+$, and B220$^+$ when mixed 1:10 WT/*Hem1*$^{+/-}$, indicating that the inability of *Hem1*$^{-/-}$ cells to contribute is not because of allorejection by WT cells (Fig. S5).

We next determined the ability of Hem1-deficient progenitor cells to reconstitute the B cell lineage in either unirradiated (Fig. 5 B) or lethally irradiated *Rag2*$^{-/-}\gamma c^{-/-}$ hosts (Fig. S5). As shown in Fig. 5 B, *Rag2*$^{-/-}\gamma c^{-/-}$ mice are completely blocked in B cell development at the B220$^+$IgM$^-$ pro–B cell stage (columns 1 and 2). Lin$^-$CD45.1$^+$ WT progenitors reconstitute B220$^+$IgM$^+$ cells in the BM and spleen of *Rag2*$^{-/-}\gamma c^{-/-}$ hosts (Fig. 5 B, column 3). In contrast, Lin$^-$CD45.2$^+$ *Hem1*$^{-/-}$ progenitors fail to generate mature B cells in unirradiated *Rag2*$^{-/-}\gamma c^{-/-}$ hosts (Fig. 5 B, column 4), despite partial reconstitution of mature T cells (Fig. 5 A). However, *Hem1*$^{-/-}$ progenitors can generate a small population of mature B cells when transplanted into lethally irradiated *Rag2*$^{-/-}\gamma c^{-/-}$ hosts (Fig. S5). WT, but not *Hem1*$^{-/-}$ progenitors, develop normally into B cells when mixed 1:1 or 1:10 with Hem1-deficient progenitors before transplantation into *Rag2*$^{-/-}\gamma c^{-/-}$ hosts (Fig. 5 B, columns 5 and 6; and Fig. S5). These results suggest that Hem1 plays an important role in the development and/or homeostasis of lymphocytes.

### Loss of Hem1 inhibits T cell activation and proliferation and enhances IL-17 production

We next examined whether loss of Hem1 affects T cell activation and T helper differentiation. We find that Hem1 deficiency results in impaired T cell activation based on reduced CD69 expression (Fig. 6 A and Fig. S6, available at http://www.jem.org/cgi/content/full/jem.20080340/DC1), decreased cell division as assessed by limited CFSE dye dilution of live-gated cells (Fig. 6 B and Fig. S6), and reduced tritiated thymidine incorporation (Fig. S6) after TCR stimulation. However, IL-2 and IFN-γ are produced normally by *Hem1*$^{-/-}$ T cells after TCR stimulation (Fig. 6, C and E), and exogenous IL-2 does not rescue proliferation of *Hem1*$^{-/-}$ T cells after α–CD3-ε/CD28 stimulation (Fig. 6 B). These results suggest that the inability of *Hem1*$^{-/-}$ T cells to divide is not because of the inability to make IL-2. Surprisingly, *Hem1*$^{-/-}$ T cells produce 15-fold more IL-17 and twofold more IL-6 and TNF-α after α-CD3/CD28 stimulation, compared with their WT counterparts (Fig. 6 C), and contain increased serum IL-17 and IL-6 in vivo (Fig. S6). Purified CD4 T cells also contain a greater percentage of Th17 effector cells after in vitro stimulation, as assessed by intracellular staining with α–IL-17 and α–IL-2 antibodies (Fig. S7). To assess whether Hem1 might modulate Th17 differentation, we purified naive WT and *Hem1*$^{-/-}$ CD4 T cells and subjected them to Th1 or Th17 polarizing conditions in the presence of irradiated APCs. We find that Th1 differentiation occurs normally in the absence of Hem1 based on an equivalent percentage of IFN-γ–producing cells (Fig. S7) and equivalent IFN-γ production (Fig. 6 E) from *Hem1*$^{-/-}$ and WT CD4 T cells after Th1 culture conditions. In contrast, the generation of Th17 cells is enhanced after IL-17 polarizing conditions with the addition of TGF-β (Figs. 6 D). It is unlikely that the skewing toward Th17 cells is caused by secondary infections because we only occasionally find histological evidence of infection in *Hem1*$^{-/-}$ mice, and *Hem1*$^{-/-}$ mice treated with antibiotics throughout their lives still produce increased IL-17 (Fig. S7).

### Hem1 is required for formation of the WAVE complex and F-actin polymerization

To determine how loss of Hem1 results in defective T cell activation and proliferation, we examined whether F-actin polymerization is altered in *Hem1*$^{-/-}$ T cells. Thymocytes and peripheral T cells were stimulated with α–CD3-ε/CD28 for 24 h, followed by PMA/Ionomycin for 15 min, and then stained with Alexa Fluor 488–conjugated phalloidin. Both *Hem1*$^{-/-}$ thymocytes (Fig. 7 A) and T cells (not depicted) fail to polymerize F-actin after α–CD3-ε/α-CD28 stimulation, relative to WT thymocytes and T cells. *Hem1*$^{-/-}$ T cells also fail to form synapse-like actin cap structures after stimulation with α–CD3-ε-coated beads (Fig. 7 B). Thymocytes and T cells from *Hem1*$^{-/-}$ mice exhibit reduced integrin-mediated cell adhesion to fibronectin after TCR stimulation, relative to WT cells (Fig. 7 C). These results suggest an essential role for Hem1 in cytoskeletal reorganization and cell adhesion at the immune synapse.

We next asked at what point Hem1 deficiency impinges on the signaling pathways leading to F-actin polymerization in lymphocytes and neutrophils. *Hem1*$^{-/-}$ thymocytes and T cells express normal levels of the membrane-proximal signaling molecules CD3-ε (not depicted), Lck, Zap70, and Rac1 (Fig. 7 D, right). In addition, we observe equivalent levels of total phosphotyrosine, active (phospho) extracellular regulated mitogen-activated protein kinase (Erk), and active Rac1 (Pak1 binding) in WT and *Hem1*$^{-/-}$ thymocytes, T cells stimulated with

α–CD3-ε (Fig. 7 D), and neutrophils stimulated with MLP (Fig. 7 E), suggesting that membrane proximal signaling is intact. *Hem1*$^{-/-}$ CD4 T cells also exhibit normal nuclear translocation of NF-κB (active NF-κB) after TCR stimulation and slightly increased basal NF-κB translocation before stimulation relative to WT CD4 T cells, as measured using ImageStream quantitative flow cytometry (Fig. S7) (31, 32). However, analysis of whole cell lysates from WT and *Hem1*$^{-/-}$ thymocytes, T cells, and neutrophils indicates that loss of Hem1 results in the near complete absence of the WAVE complex proteins Wave2, Abi1, Abi2, and Sra1 in thymocytes and purified T cells (Fig. 7 F, left and middle), whereas WAVE members are reduced in *Hem1*$^{-/-}$ neutrophils (Fig. 7 F, right). The reduction in WAVE complex proteins is not caused by decreased transcription

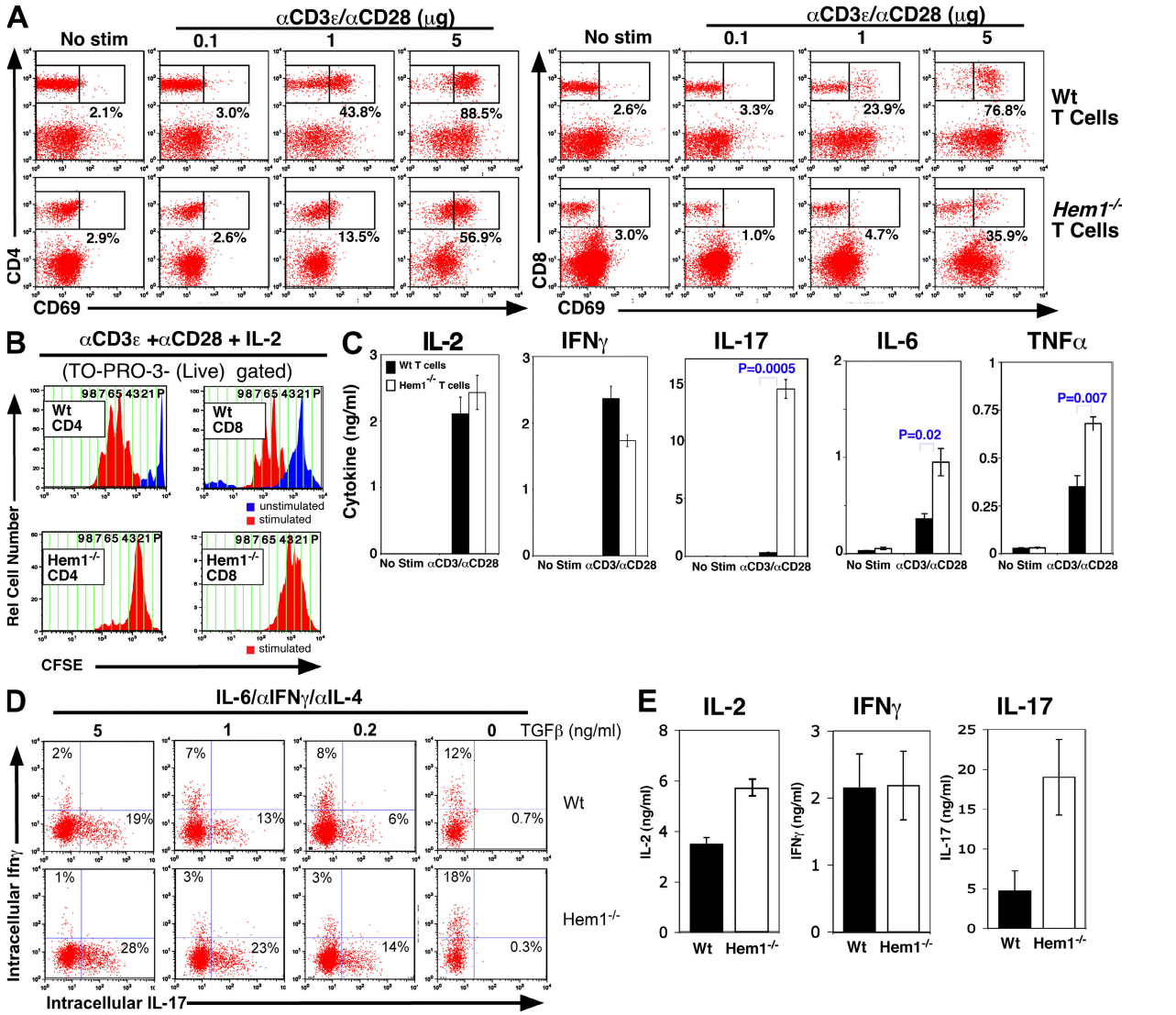


**Figure 6. Loss of Hem1 results in enhanced IL-17 production but normal IL-2 and IFN-γ production (A) Splenocytes from WT and *Hem1*$^{-/-}$ mice were stimulated with different doses of α-CD3/α-CD28 for 18 h.** Cells were stained with fluorescent-conjugated α-CD4, α-CD8, and α-CD69 and analyzed by flow cytometry. Representative dot-plot histograms of three independent experiments are shown. (B) Purified WT and *Hem1*$^{-/-}$ T cells were labeled with CFSE dye and were stimulated with α-CD3/CD28 in presence of IL-2 for 4 d. Cells were stained with α-CD4, α-CD8, and the vital dye TO-PRO-3. Cell divisions were determined by flow cytometry on live-gated (TO-PRO-3 negative) CD4$^+$ or CD8$^+$ cells. Representative single-parameter histograms of three independent experiments are shown (each division is separated by vertical lines). Because of the paucity of peripheral T cells in *Hem1*$^{-/-}$ mice, all purified T cells from *Hem1*$^{-/-}$ mice are used for the stimulated condition. (C) Splenic T cells were stimulated with α-CD3/α-CD28 for 72 h. Culture media were harvested and IL-2, IFN-γ, IL-17, IL-6, and TNF-α production were measured by ELISA. Error bars represent the mean ± SEM of three mice per group. P-values are shown. (D) FACs-sorted CD4$^+$CD25$^-$CD44$^{low}$CD62L$^+$ naive T cells from WT and *Hem1*$^{-/-}$ mice were cultured for 5 d under the indicated conditions (Th17), followed by intracellular staining for IL-17 and IFN-γ. A representative dot-plot histogram of three independent experiments is shown. (E) After 5-d culture under Th1 or Th17 conditions, cells were restimulated with α-CD3 and secreted cytokines were measured by ELISA. Data were obtained from two independent experiments. Error bars show the mean ± SEM.

because *Abi1*, *Abi2*, *Sra1*, and *Wave2* mRNA are expressed normally in *Hem1*$^{-/-}$ T cells relative to WT T cells (Fig. S8). In addition, acute small inhibitory RNA (siRNA) knockdown (33) of *Hem1* in WT T cells in vitro results in decreased amounts of Wave2, Abi2, and Sra1 (Fig. S8). These results suggest that Hem1 is required for stabilization and/or translation of the WAVE complex proteins in hematopoietic cells (Fig. 8), and they are consistent with several recent studies indicating that siRNA knockdown of Hem1 in HL-60 cells (25) or Jurkat T cells (34) results in degradation of WAVE complex proteins, which are essential mediators of F-actin polymerization.

## DISCUSSION

Reorganization of the actin cytoskeleton is implicated in many active cellular processes in hematopoietic cells including

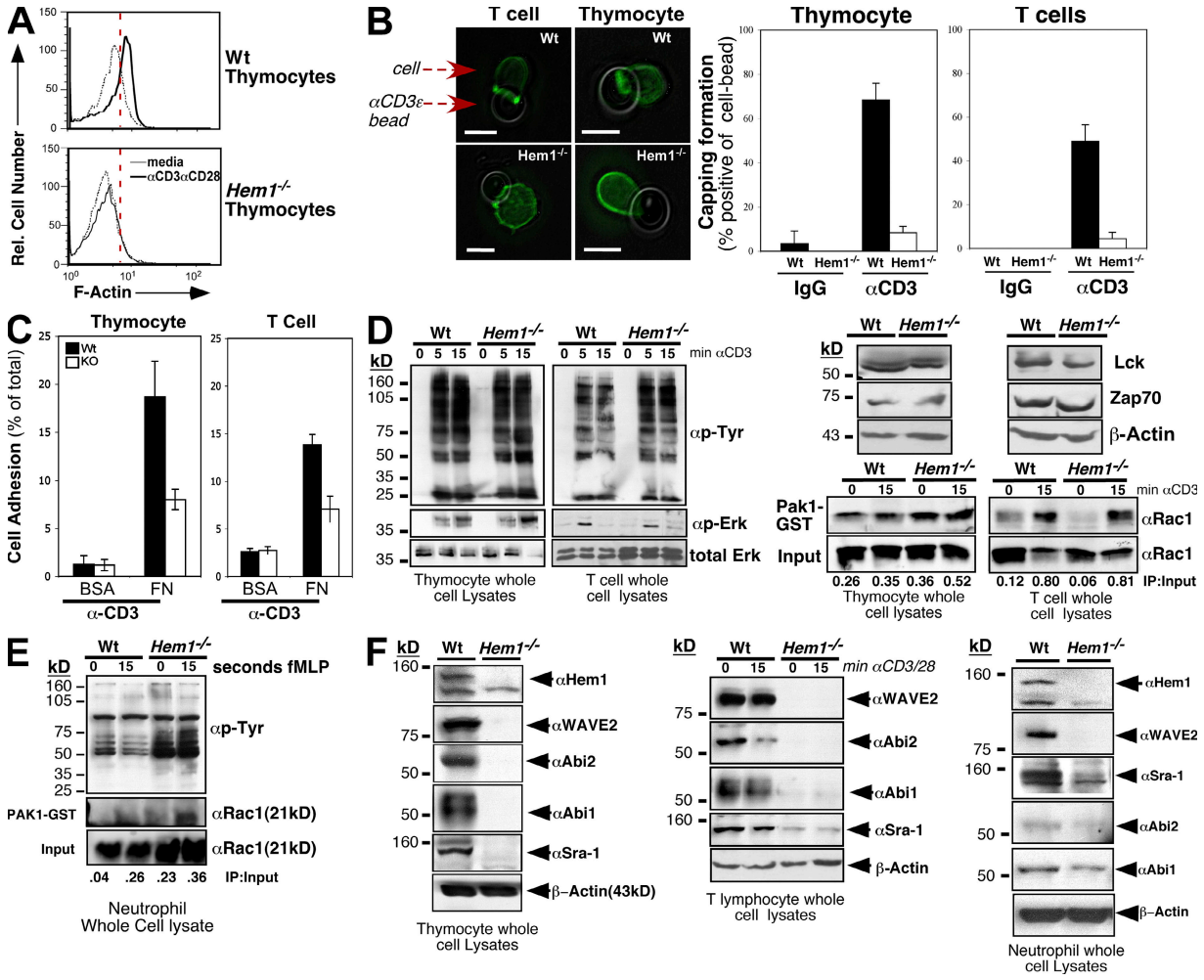


**Figure 7. Loss of Hem1 results in defective F-actin polymerization and actin cap formation, impaired cell adhesion, and loss of WAVE complex components.** (A) Thymocytes from WT and *Hem1*$^{-/-}$ mice were stimulated with α-CD3/α-CD28 for 24 h, followed by PMA for 15 min. Cells were stained with Alexa Fluor 488 phalloidin, and F-actin polymerization was measured by flow cytometry. A single-parameter histogram, representative of three experiments, is shown. (B) *Hem1*$^{-/-}$ T cells display defective TCR-induced capping formation and adhesion. Thymocytes or T cells were incubated with hamster IgG- or α–CD3-ε-coated beads for 30 min and then stained with Alexa Fluor 488 phalloidin and analyzed by confocal microscopy. (B, left) A representative image of capping formation between the T cells or thymocytes and beads. Bars, 5 µm. (B, right) The percentages of positive cell–bead contacts are graphed. Results are representative of two independent experiments. The mean ± SEM is shown. (C) Defective adhesion capacity of *Hem1*$^{-/-}$ T cells. Thymocytes and T cells were incubated on fibronectin-coated plates and stimulated with α-CD3 for 30 min. Results are representative of two independent experiments. The mean + SEM is shown. (D–F) Loss of WAVE components in *Hem1*$^{-/-}$ hematopoietic cells. Thymocytes and T cells from WT and *Hem1*$^{-/-}$ mice were stimulated on α-CD3–coated plates for the indicated time points, and neutrophils were stimulated with MLP for 0 and 15 s. Cells were lysed and subjected to Western blot analysis using antibodies against Hem1, Lck, Zap70, Wave2, Sra1, Abi1, Abi2, β-Actin, phosphotyrosine, total Erk, and phospho-Erk. To assess the Pak1 binding activity of activated Rac proteins, cell extracts from either WT or *Hem*$^{-/-}$ mice were incubated as described in Materials and methods. Active Rac proteins were analyzed by Western blotting with α-Rac antibodies. The relative ratio of Rac1 in the immunoprecipitation relative to input is shown below each blot. There is no significant difference in Rac1 activity in *Hem1*$^{-/-}$ versus WT samples (time 0, P = 0.2; 15 min, P = 0.09). Blots are representative of three independent experiments.

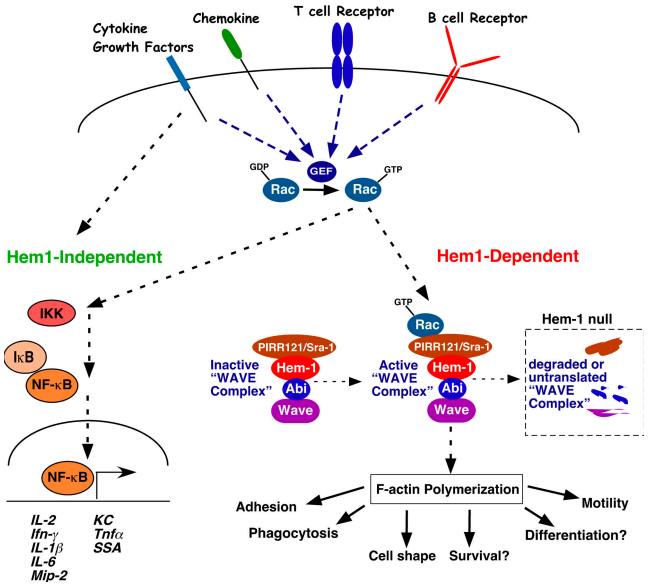


**Figure 8. Model of Hem1 functions in F-actin polymerization and hematopoietic cell biology.** In mammalian cells, the WAVE complex consists of multiple subunits including WAVE (1, 2, or 3), Abi (1 or 2), Hem (Hem2 [also known as Nap 1] or Hem1), and Sra1 (19). The WAVE complex alone does not induce actin polymerization but is stimulated in response to Rac GTP, which is activated by many receptors, and is brought into the WAVE complex via associations with Sra1 and Hem. Hem1 is the essential Hem family member in hematopoietic cells. Association of Rac GTP with WAVE may lead to WAVE-induced activation or relocalization of the actin-regulatory protein complex (not depicted), resulting in F-actin polymerization. Hem1 deficiency results in loss of WAVE complex proteins, thus specifically blocking processes dependent on F-actin polymerization, whereas Rac GTP activation of NF-κB–dependent transcription proceeds normally.

cell adhesion, migration, homing, phagocytosis, and proliferation. However, the specific signaling molecules and pathways that regulate the actin cytoskeleton in hematopoietic cells in vivo are unclear. In this study, we used a phenotype-driven ENU mutagenesis strategy in mice to identify a novel loss-of-function mutation in *Hem1*. Our studies reveal that Hem1 is an essential hematopoietic cell-specific regulator of the actin cytoskeleton, where it controls cell migration, adhesion, phagocytosis, and proliferation. Importantly, this study supports the utility of using ENU mutagenesis to generate immunodeficiency models in mice caused by single-point mutations, which more closely mimic the genetic alterations that result in human genetic diseases (35, 36). The relative hematopoietic cell-specific expression of *Hem1*, and the multilineage immunodeficiency phenotype of *Hem1*-deficient mice, suggests that a subset of immunodeficiency diseases in humans may include loss-of-function mutations in *Hem1*.

Analysis of *Hem1*$^{-/-}$ mice reveals a severe defect in the development and expansion of αβ T cells, predominantly at the DN-to-DP cell transition. Further examination of gated DN populations by flow cytometry indicates that *Hem1*-deficient thymocytes are inhibited at the CD25$^{+}$CD44$^{-}$ DN3 to CD25$^{-}$CD44$^{-}$ DN4 cell stage, mediated by formation of the pre-TCR complex. Although Rac activation appears normal in *Hem1*$^{-/-}$ thymocytes, F-actin polymerization and T cell capping are completely lost, and components of the WAVE complex disappear in the absence of Hem1. These results suggest that Hem1 has an essential role in T cell development and F-actin polymerization, perhaps by stabilizing the WAVE complex downstream of Rho family members. Our results extend a previous series of elegant studies suggesting that the Rac GTP exchange factor Vav1 (37, 38), as well as Rac (14) and Rho (16, 39, 40), are essential for T cell development at the DN-to-DP cell transition by regulating cell survival. Indeed, we also find an increased incidence of apoptosis in *Hem1*$^{-/-}$ thymocytes and mature T cells (Fig. S6). The generation of T cell–specific *Hem1*-deficient mice will be required to more clearly delineate the involvement of Hem1 in pre-TCR signaling and to separate specific and potentially nonspecific contributions of Hem1 deficiency on T cell development.

Previous studies have also suggested that the actin-regulatory proteins Vav (see (41) for review), Rho (15), Rac (3), HS1 (42), Dynamin (43), Abi1/2 (44), and WAVE2 (34) have essential roles in T cell activation by regulating actin reorganization, immune synapse formation, and calcium signaling. In addition, Rac2 has been shown to regulate Th1 cell differentiation by inducing the IFN-γ promoter through the cooperative activation of the NF-κB and p38 mitogen-activated protein kinase pathways (4). We find that loss of Hem1 impairs T cell activation based on decreased CD69 up-regulation and decreased cell division of live-gated cells after α-CD3/α-CD28 stimulation. In addition, we find a defect in F-actin polymerization, actin capping, and cell adhesion in Hem1-deficient thymocytes and T cells. However, in contrast to loss of Vav1 (45), WASp (46), and Rac2 (3), we find that loss of Hem1 does not affect TCR-induced calcium signaling (unpublished data) and IL-2 production, nor is cell proliferation rescued by the addition of IL-2. In addition, we find that IFNγ, IL-6, and TNF-α production occurs normally in *Hem1*$^{-/-}$ T cells. The differences between loss of Vav1 and Rac2 versus loss of Hem1 likely reflect a bifurcation of signals from Vav1 and Rac2 upstream of Hem1. Consistent with this notion, we find that loss of Hem1 specifically disrupts processes that are dependent on actin reorganization, such as cell migration, adhesion, and immune synapse formation, whereas NF-κB–dependent transcription of IL-2, IFN-γ, and proinflammatory cytokines proceed normally.

Loss of Vav1 (47) and Rac (17) have also been shown to be essential for normal B cell development and signaling by regulating cell survival. In addition, high *Hem1* expression has recently been associated with a poor clinical outcome in B cell chronic lymphocytic leukemia, and down-regulation of *Hem1* by antisense treatment increased susceptibility of chronic lymphocytic leukemia cells to fludarabine-mediated killing (48). Our results show that Hem1 is essential for both B and T cell development, and they are consistent with Hem1 acting downstream of Vav and Rac during lymphocyte development. These results collectively suggest that Hem1-deficient

mice provide an important resource to examine the importance of Hem1 in transformation and metastasis of hematopoietic cancers.

Innate immune responses are dependent on the ability of phagocytic cells to sense invading microbes through Toll-like receptors and to respond to chemoattractant molecules by migrating to inflammatory sites, where they produce proinflammatory cytokines and phagocytose and kill invading pathogens. Our analyses of blood and BM from *Hem1*$^{-/-}$ mice reveal severe but distinct alterations in innate immune responses associated with Hem1 deficiency. Purified neutrophils and macrophages from *Hem1*$^{-/-}$ mice fail to phagocytose bacteria, and mutant neutrophils fail to migrate across a membrane and polymerize F-actin in response to stimulation. Neutrophil numbers are increased up to 25-fold in peripheral blood from *Hem1*$^{-/-}$ mice, which is consistent with decreased migration in vivo. The neutrophilic response in *Hem1*$^{-/-}$ mice also correlates with increased numbers of proinflammatory Th17 cells, increased serum IL-17 and IL-6, and increased production of IL-1β, Mip-2, and KC from in vitro–stimulated macrophages. Because IL-17 potently stimulates the expansion and chemotaxis of neutrophils in a G-CSF–dependent manner (49), the neutrophilic phenotype seen in *Hem1*$^{-/-}$ mice may result from increased Th17 effector cells. Likewise, the increased serum amyloid A from liver cells (which is made in response to IL-1, IL-6, and TNF-α) is likely the source of the amyloid deposits seen in *Hem1*$^{-/-}$ liver, kidney, and heart (Fig. 2 G and Fig. S6). Although the exact mechanism is unclear, the increase in Th17 effector cells in *Hem1*$^{-/-}$ mice may be caused by the following: impaired neutrophil migration into tissues combined with defective phagocytosis of tissue neutrophils by macrophages, which could result in increased production of IL-23 from tissue macrophages (Fig. S3) (50); increased Th17 differentiation from naive T cells (Fig. 6 and Fig. S7) in response to increased IL-6 (Fig. 6 and Fig. S6) and ICOS (Fig. S7); and/or increased production of IL-17–producing memory T cells in response to lymphopenia and impaired innate immunity.

Neutrophils from Vav1/2-deficient mice also exhibit defective adhesion, migration, and phagocytosis (51). Similarly, neutrophils from Rac2-deficient mice (7, 52), as well as a human patient with a dominant-negative RAC2 mutation (8), exhibit impaired neutrophil migration and phagocytosis. Although *Hem1*$^{-/-}$ neutrophils exhibit normal Rac activation, components of the Rac-effector WAVE complex are severely reduced after loss of Hem1. These results are consistent with Hem1 acting downstream of Rac to stimulate actin polymerization in neutrophils, perhaps by stabilizing the WAVE complex. However, although macrophages from *Hem1*$^{-/-}$ mice are also defective in their ability to phagocytose bacteria, they produce normal or increased amounts of the proinflammatory cytokines and chemokines in response to toll-like receptor stimulation. Hence, as we observed in T cells, our results suggest that NF-κB–mediated transcription of proinflammatory cytokines proceeds independently of Hem-1 in phagocytes. The imbalance between a functional proinflammatory cytokine arm and dysfunctional effector arm in both lymphocytes and phagocytes from *Hem1*$^{-/-}$ mice may explain the unique pathology after loss of Hem1. Altogether, our results suggest that Hem1 is essential for innate immune cell function and homeostasis by regulating F-actin polymerization.

Rac1 and Rac2 also regulate many aspects of HSC biology, including adhesion, migration, mobilization, and engraftment. Indeed, we also find that Hem1 deficiency results in decreased colony-forming activity in the BM and increased colony-forming activity in the spleen and peripheral blood, and *Hem1*$^{-/-}$ Lin$^{-}$ cells compete poorly with WT Lin$^{-}$ cells after BM transplantation. These results are consistent with decreased adhesion of HSC/Ps in the BM niche, resulting in their release (mobilization) into peripheral blood and spleen of *Hem1*$^{-/-}$ mice (10), as is seen in Rac-deficient mice (11, 53). Additional experimentation will be required to definitively determine whether Hem1 also regulates HSC survival and proliferation.

Hem family proteins are highly conserved across Phyla. Disruption of specific Hem family orthologues in *D. discoideum* (24), *D. melanogaster* (54), and *C. elegans* (22) reveal a common theme of defective development, failed migration of embryonic tissues, and disrupted morphogenesis, all of which correlate with impaired actin reorganization. Similarly, the recent disruption of *Nap1* (*Hem2*) in mice results in early embryonic lethality caused by impaired neuronal differentiation and outgrowth, whereas premature retroviral expression of *Nap1* promotes postmigratory differentiation (26). Our results indicate that Hem1 is the key Hem family member in hematopoietic cells, where it controls lymphocyte development and activation, as well as phagocyte function. The finding that Hem1 is relatively restricted to hematopoietic cell types, and that it plays a key role in actin reorganization (55) and survival of both normal and transformed cells, suggests that Hem1 might prove to be a valuable drug target in inflammatory diseases or cancer.

## MATERIALS AND METHODS

**ENU mutagenesis, screening, and mutation mapping.** Mutagenesis with ENU was performed on C57BL/6J male mice according to the protocol used by Justice et al. (56). Two mating schemes were used. G2 NTB.1 carriers were crossed to C3HeB/FeJ and the resulting F1 animals were intercrossed to generate F2 animals for mapping. In addition, the G1 NTB.1 carrier was mated to C3HeB/FeJ mice and the resulting F1 animals were backcrossed to the G1 carrier to generate N2 mice for mapping. F2 and N2 animals were screened for the NTB.1 trait and DNA was collected. DNA was analyzed with 85 microsatellite markers spaced a mean of 15 cM apart. Linkage analysis was performed using MapManager QTX13b software (K. Manly, Roswell Park, Buffalo, NY). The ∼360-kb *NTB.1* candidate interval was narrowed between 59.8 and 60.1 cM on chromosome 15. Computational analysis identified 11 genes, whose exons were PCR amplified from genomic DNA and sequenced.

**Mice.** *Hem-1* mutant mice were housed under specific pathogen-free conditions. Mouse procedures were approved by the Institutional Animal Care and Use Committees of Celltech R&D, Inc., and the University of Washington. The NTB.1 line was screened and maintained by DNA sequencing after amplification with *Hem1* forward (5′-TGCAGAGCTTCTGTTCCTGTTGGA-3′) and reverse (5′-AGAAGGAACTGCTGGCTACCCAAA-3′) primers and by flow cytometry comparing the ratio of B220$^{low}$ to Gr-1$^{high}$

cells. The majority of the phenotypic analysis of *Hem1*$^{-/-}$ mice was performed on intercrosses between mice backcrossed three generations onto C57BL6J (from the original C57BL6J × C3H hybrids).

**Generation of neutrophils by in vitro cell culture.** Single-cell suspensions of BM cells were cultured in 6-well culture dishes at 2 × 10$^6$ cells/ml. Cells were grown with DMEM/20% FBS medium in the presence of IL-3/GM-CSF (28). After 3 d, nonadherent cells were removed, and adherent cells were continuously grown with IL-3/GM-CSF. After an additional 10 d, nonadherent cells were used in the experiments after initiation of the culture. Nonadherent cells were stained with Gr-1/Mac1 and analyzed by flow cytometry.

**Erythrocyte osmotic fragility assay.** Blood was obtained from WT and *Hem1*$^{-/-}$ mice and diluted 1:1,000 in PBS containing EDTA for the cell counting. 20 × 10$^6$ erythrocytes in 100 µl (0.9% NaCl) were dropped into solutions containing either 0.9% saline or a hypotonic solutions to generate final NaCl concentrations of 0.86, 0.74, 0.69, 0.47, or 0.26% NaCl. In brief, erythrocyte samples were slowly dropped (without mixing) into 250-µl NaCl solutions, incubated for 10 min, and then centrifuged for 1 min at 1,300 rpm. The supernatant was analyzed for released hemoglobin by measuring the absorbance at 540 nm. Samples were normalized to a standard curve generated from complete lysis (100% lysis) and zero lysis (0.9% NaCl) for each of the mice (57).

**Generation of BM chimeras.** *Rag2*$^{-/-}\gamma c^{-/-}$ mice (Taconic) were reconstituted with *Hem1*$^{-/-}$ (KO; CD45.2) or C57BL/6J WT (CD45.1; Jackson ImmunoResearch Laboratories) Lin$^-$ cells or mixed populations of Lin$^-$ or total BM cells (WT:*Hem1*$^{-/-}$, 1:1, 1:10, or 1:20). Lineage$^+$ cells were depleted using the Mouse lineage panel kit (BD) according to manufacturer's instructions. Lin$^-$ cells (2 × 10$^4$ cells/each) were injected i.v. into nonirradiated or 950 rad–irradiated *Rag2*$^{-/-}\gamma c^{-/-}$ recipients. In other experiments, total BM cells depleted of CD3$^+$ cells were used for BM chimera studies. Thymus, BM, and spleen cells were collected from the recipient mice 6–20 wk after reconstitution.

**Rac activation assay.** The EZ-Detect Rac1 activation kit (Thermo Fisher Scientific) was used to pull down active Rac1. The PAK1-bound active Rac1 was detected by Western blot analysis (52) using α-Rac1 antibody (BD) and visualized using the ODYSSEY infrared imaging system (LI-COR Biosciences) located at the Fred Hutchinson Cancer Research Center (Seattle, WA).

**Neutrophil purification and chemotaxis assays.** Neutrophils were purified from WT and *Hem1*$^{-/-}$ BM using Histopaque 1119 and 1077 gradients (Sigma-Aldrich). Chemotaxis assays were conducted according to a protocol provided by Neuro Probe, Inc. The number of migrated cells per 400× field were counted for three random spots and mean values were displayed on the y axis (6).

**In vitro phagocytosis assay.** Neutrophils or peritoneal macrophages (10$^5$ cells) were incubated with fluorescent beads (Polysciences, Inc.) or fluorescent *E. coli* (Invitrogen) for 0, 2, and 4 h. The intensity of phagocytosed beads or *E. coli* was then analyzed by flow cytometry.

**Measurements of cytokines and chemokines.** Cytokines (IL-2, IFN-γ, IL-17, IL-6, IL-1β, and TNF-α) and chemokine (MIP2 and KC) levels were quantified with capture/detection antibody-based ELISA systems (eBioscience; R&D Systems), according to the manufacturer's instructions. IL-17 in sera from WT and *Hem1*$^{-/-}$ mice was assessed using a Biosource (Invitrogen) mouse IL-17 antibody bead kit according to the manufacturer's recommendations. In brief, 100 µl of sera were incubated with fluorescent beads conjugated to the capture antibody. After addition of the detection antibody mix and PE-conjugated streptavidin, plates were read on a LUMINEX machine using xMAP technology (QIAGEN).

**Cell adhesion assay.** Flat-bottom Maxisorb 96-well plates were coated with 0.5 µg/ml of human fibronectin (BD) and bovine serum albumin (Sigma-Aldrich). Cells were added to the wells, stimulated with α–CD3-ε, washed, and counted under an inverted microscope as previously described (11).

**Capping formation, immunofluoresence, and confocal microscopy.** Thymocytes from WT and *Hem1*$^{-/-}$ mice were stimulated with α-CD3/α-CD28 for 24 h, followed by PMA for 15 min. Cells were fixed, permeabilized, and stained with Alexa Fluor 488 phalloidin. F-actin polymerization and actin capping formation were determined by flow cytometry and confocal microscopy after phalloidin–Alexa Fluor 488 and DAPI staining, as previously described (3, 7). Hamster IgG– or α–CD3-ε-coated 5-µm sulfate white microspheres were prepared according to the manufacturer's protocol (Invitrogen).

**T cell isolation and Th differentiation.** CD4$^+$CD44$^{low}$CD25$^-$CD62L$^+$ T cells (4 × 10$^4$ cells) sorted using FACS Vantage or FACS Aria (BD) were activated with plate-bound 1 µg/ml α-CD3 and irradiated APC (10$^5$ cells, 3,000 rads) in the presence of 10 ng/ml IL-12 (R&D Systems), 10 µg/ml α–IL-4 antibody (11B11; eBioscience), and 5 ng/ml IL-2 (R&D Systems) for Th1 differentiation condition, as previously described (4). For Th17 differentiation conditions, different doses of TGF-β (5, 1, 0.2, and 0 ng/ml; R&D Systems), IL-6 (50 ng/ml, R&D Systems), α–IL-4 (10 µg/ml), and α–IFN-γ (10 µg/ml) antibodies were added to culture media (58).

**Western blot analysis.** Western blot analyses were performed as previously described (59) using rabbit polyclonal antibodies specific for Hem1 (gift from O.D. Weiner, University of California, San Francisco, San Francisco, CA), β-actin (Santa Cruz Biotechnology, Inc.), Wave2 (Santa Cruz Biotechnology, Inc.), Abi1 (Santa Cruz Biotechnology, Inc.), Abi2, and Sra1 (gifts from A.M. Pendergast [Duke University, Durham, NC] and J.D. Scott [University of Washington, Seattle, WA]), Lck, Zap70 (Millipore), and donkey α–goat IgG HRP (Santa Cruz Biotechnology, Inc.), goat α–rabbit IgG HRP (Bio-Rad Laboratories), goat α–mouse IgG HRP (Bio-Rad Laboratories), 4G10 antibody (Millipore), Phospho-Erk, and total Erk (Cell Signaling Technology) (38).

**Histology and hematology.** Tissues were embedded in paraffin and stained with hematoxylin and eosin (Histology Consultation Services, Inc.). CBCs were performed by Phoenix Central Laboratory (Everett, WA).

**T cell proliferation.** T cells (10$^6$ cells/ml) were labeled with CFSE dye (10 µM; Invitrogen) and stimulated with α-CD3/α-CD28 in the presence of 10 ng/ml IL-2 (R&D Systems) for 4 d. Cell divisions were determined in 1 nM of live TO-PRO-3 (Invitrogen) and negative cells were determined by flow cytometry, as previously described (59). In addition, cells were labeled with $^3$H thymidine for 18 h, and cell proliferation was determined as previously described (60).

**Flow cytometry and cell sorting.** *Hem1*$^{-/-}$ and WT tissues (BM, thymus, spleen, and LN) were stained with fluorescent-conjugated antibodies specific for CD8, GR1, B220 (Invitrogen), CD62L, Sca1, cKit, Foxp3, IL-2, IL-17, IFN-γ (eBioscience), CD4, CD3-ε, CD69, CD43, ICOS, IgM, MAC1, GR1, Ter119, CD61, CD45.1, CD45.2, Annexin V, CD44, CD25, β-TCR, γδ-TCR, BP1, and heat stable antigen (BD) and analyzed by flow cytometry as previously described (59, 60). To purify enriched HSC/Ps, Lin$^-$ cells were then sorted based on expression of ckit (CD117), Sca1 (Ly-6A/E), and Hoechst 33342 (Invitrogen) to define SP cells (61).

**Statistical analysis.** Data were analyzed using the Student's one-tailed *t* test. P-values < 0.05 were considered as significant values.

**Online supplemental material.** Fig. S1 shows that the *Hem1* gene is preferentially expressed in lymphoid tissues and HSC. Fig. S2 shows decreased clonogenic hematopoietic cell potential in the BM and increased clonogenic hematopoietic cell potential in the blood and spleen in *Hem1*$^{-/-}$ mice. Fig S3 shows that *Hem1*$^{-/-}$ peritoneal macrophages produce normal or increased

levels of proinflammatory cytokines in response to toll-like receptor signaling. Fig. S4 shows that transfection of *Hem1* plasmid rescues F-actin formation in *Hem1*$^{-/-}$ granulocytes. Fig. S5 shows that *Hem1*$^{-/-}$ BM cells compete poorly with WT BM cells after transfer into irradiated *Rag2*$^{-/-}$/$\gamma c^{-/-}$ mice. Fig. S6 shows that loss of Hem1 impairs T cell proliferation and survival, whereas proinflammatory cytokine production is increased. Fig. S7 shows that *Hem1*$^{-/-}$ mice produce increased IL-17 and exhibit normal or increased NF-κB activation. Fig. S8 shows that components of the WAVE complex are transcribed normally in *Hem1*$^{-/-}$ mice, and siRNA knockdown of *Hem1* in WT T cells results in decreased amounts of WAVE complex proteins. Online supplemental material is available at http://www.jem.org/cgi/content/full/jem.20080340/DC1.

We thank Leslie Wilson for assistance with mouse genotyping and colony management; Orion Weiner, Ann Marie Pendergast, and J.D. Scott for generously providing antibodies; and Yansong Gu for assistance with confocal microscopy.

This study was supported in part by National Institutes of Health grant (RO1AI0535468 to B.M.I.) and by funding from Celltech R&D, Inc, and the Department of Comparative Medicine (University of Washington, Seattle, WA).

A potential conflict of interest is that S. Friend is employed by Amnis, Inc., the company which makes the ImageStream instrument used to generate Fig. S7 E. The authors have no further competing financial interests.

**Submitted: 20 February 2008**
**Accepted: 20 October 2008**

## REFERENCES

1. Hall, A., and C.D. Nobes. 2000. Rho GTPases: molecular switches that control the organization and dynamics of the actin cytoskeleton. *Philos. Trans. R. Soc. Lond. B Biol. Sci.* 355:965–970.
2. Weston, V.J., and T. Stankovic. 2004. Rac1 and Rac2 GTPases in haematopoiesis. *Bioessays.* 26:221–224.
3. Yu, H., D. Leitenberg, B. Li, and R.A. Flavell. 2001. Deficiency of small GTPase Rac2 affects T cell activation. *J. Exp. Med.* 194:915–926.
4. Li, B., H. Yu, W. Zheng, R. Voll, S. Na, A.W. Roberts, D.A. Williams, R.J. Davis, S. Ghosh, and R.A. Flavell. 2000. Role of the guanosine triphosphatase Rac2 in T helper 1 cell differentiation. *Science.* 288:2219–2222.
5. Benvenuti, F., S. Hugues, M. Walmsley, S. Ruf, L. Fetler, M. Popoff, V.L. Tybulewicz, and S. Amigorena. 2004. Requirement of Rac1 and Rac2 expression by mature dendritic cells for T cell priming. *Science.* 305:1150–1153.
6. Carstanjen, D., A. Yamauchi, A. Koornneef, H. Zang, M.D. Filippi, C. Harris, J. Towe, S. Atkinson, Y. Zheng, M.C. Dinauer, and D.A. Williams. 2005. Rac2 regulates neutrophil chemotaxis, superoxide production, and myeloid colony formation through multiple distinct effector pathways. *J. Immunol.* 174:4613–4620.
7. Roberts, A.W., C. Kim, L. Zhen, J.B. Lowe, R. Kapur, B. Petryniak, A. Spaetti, J.D. Pollock, J.B. Borneo, G.B. Bradford, et al. 1999. Deficiency of the hematopoietic cell-specific Rho family GTPase Rac2 is characterized by abnormalities in neutrophil function and host defense. *Immunity.* 10:183–196.
8. Williams, D.A., W. Tao, F. Yang, C. Kim, Y. Gu, P. Mansfield, J.E. Levine, B. Petryniak, C.W. Derrow, C. Harris, et al. 2000. Dominant negative mutation of the hematopoietic-specific Rho GTPase, Rac2, is associated with a human phagocyte immunodeficiency. *Blood.* 96:1646–1654.
9. Cancelas, J.A., M. Jansen, and D.A. Williams. 2006. The role of chemokine activation of Rac GTPases in hematopoietic stem cell marrow homing, retention, and peripheral mobilization. *Exp. Hematol.* 34:976–985.
10. Cancelas, J.A., A.W. Lee, R. Prabhakar, K.F. Stringer, Y. Zheng, and D.A. Williams. 2005. Rac GTPases differentially integrate signals regulating hematopoietic stem cell localization. *Nat. Med.* 11:886–891.
11. Gu, Y., M.D. Filippi, J.A. Cancelas, J.E. Siefring, E.P. Williams, A.C. Jasti, C.E. Harris, A.W. Lee, R. Prabhakar, S.J. Atkinson, et al. 2003. Hematopoietic cell regulation by Rac1 and Rac2 guanosine triphosphatases. *Science.* 302:445–449.
12. Yang, F.C., S.J. Atkinson, Y. Gu, J.B. Borneo, A.W. Roberts, Y. Zheng, J. Pennington, and D.A. Williams. 2001. Rac and Cdc42 GTPases control hematopoietic stem cell shape, adhesion, migration, and mobilization. *Proc. Natl. Acad. Sci. USA.* 98:5614–5618.
13. Wang, L., L. Yang, M.D. Filippi, D.A. Williams, and Y. Zheng. 2006. Genetic deletion of Cdc42GAP reveals a role of Cdc42 in erythropoiesis and hematopoietic stem/progenitor cell survival, adhesion, and engraftment. *Blood.* 107:98–105.
14. Gomez, M., V. Tybulewicz, and D.A. Cantrell. 2000. Control of pre-T cell proliferation and differentiation by the GTPase Rac-I. *Nat. Immunol.* 1:348–352.
15. Corre, I., M. Gomez, S. Vielkind, and D.A. Cantrell. 2001. Analysis of thymocyte development reveals that the GTPase RhoA is a positive regulator of T cell receptor responses in vivo. *J. Exp. Med.* 194:903–914.
16. Galandrini, R., S.W. Henning, and D.A. Cantrell. 1997. Different functions of the GTPase Rho in prothymocytes and late pre-T cells. *Immunity.* 7:163–174.
17. Walmsley, M.J., S.K. Ooi, L.F. Reynolds, S.H. Smith, S. Ruf, A. Mathiot, L. Vanes, D.A. Williams, M.P. Cancro, and V.L. Tybulewicz. 2003. Critical roles for Rac1 and Rac2 GTPases in B cell development and signaling. *Science.* 302:459–462.
18. Bustelo, X.R., V. Sauzeau, and I.M. Berenjeno. 2007. GTP-binding proteins of the Rho/Rac family: regulation, effectors and functions in vivo. *Bioessays.* 29:356–370.
19. Soderling, S.H., and J.D. Scott. 2006. WAVE signalling: from biochemistry to biology. *Biochem. Soc. Trans.* 34:73–76.
20. Hromas, R., S. Collins, W. Raskind, L. Deaven, and K. Kaushansky. 1991. Hem-1, a potential membrane protein, with expression restricted to blood cells. *Biochim. Biophys. Acta.* 1090:241–244.
21. Kunda, P., G. Craig, V. Dominguez, and B. Baum. 2003. Abi, Sra1, and Kette control the stability and localization of SCAR/WAVE to regulate the formation of actin-based protrusions. *Curr. Biol.* 13:1867–1875.
22. Soto, M.C., H. Qadota, K. Kasuya, M. Inoue, D. Tsuboi, C.C. Mello, and K. Kaibuchi. 2002. The GEX-2 and GEX-3 proteins are required for tissue morphogenesis and cell migrations in C. elegans. *Genes Dev.* 16:620–632.
23. Djakovic, S., J. Dyachok, M. Burke, M.J. Frank, and L.G. Smith. 2006. BRICK1/HSPC300 functions with SCAR and the ARP2/3 complex to regulate epidermal cell shape in Arabidopsis. *Development.* 133:1091–1100.
24. Ibarra, N., S.L. Blagg, F. Vazquez, and R.H. Insall. 2006. Nap1 regulates *Dictyostelium* cell motility and adhesion through SCAR-dependent and -independent pathways. *Curr. Biol.* 16:717–722.
25. Weiner, O.D., M.C. Rentel, A. Ott, G.E. Brown, M. Jedrychowski, M.B. Yaffe, S.P. Gygi, L.C. Cantley, H.R. Bourne, and M.W. Kirschner. 2006. Hem-1 complexes are essential for Rac activation, actin polymerization, and myosin regulation during neutrophil chemotaxis. *PLoS Biol.* 4:e38.
26. Yokota, Y., C. Ring, R. Cheung, L. Pevny, and E.S. Anton. 2007. Nap1-regulated neuronal cytoskeletal dynamics is essential for the final differentiation of neurons in cerebral cortex. *Neuron.* 54:429–445.
27. Kalfa, T.A., S. Pushkaran, N. Mohandas, J.H. Hartwig, V.M. Fowler, J.F. Johnson, C.H. Joiner, D.A. Williams, and Y. Zheng. 2006. Rac GTPases regulate the morphology and deformability of the erythrocyte cytoskeleton. *Blood.* 108:3637–3645.
28. Yamauchi, A., C.C. Marchal, J. Molitoris, N. Pech, U. Knaus, J. Towe, S.J. Atkinson, and M.C. Dinauer. 2005. Rac GTPase isoform-specific regulation of NADPH oxidase and chemotaxis in murine neutrophils in vivo. Role of the C-terminal polybasic domain. *J. Biol. Chem.* 280:953–964.
29. von Boehmer, H. 2005. Unique features of the pre-T-cell receptor alpha-chain: not just a surrogate. *Nat. Rev. Immunol.* 5:571–577.
30. Hardy, R.R., and K. Hayakawa. 2001. B cell development pathways. *Annu. Rev. Immunol.* 19:595–621.
31. Tibrewal, N., Y. Wu, V. D'Mello, R. Akakura, T.C. George, B. Varnum, and R.B. Birge. 2007. Autophosphorylation docking site Tyr867 in Mertk allows for dissociation of multiple signaling pathways for phagocytosis of apoptotic cells and down-modulation of LPS-inducible NF-kappa B transcriptional activation. *J. Biol. Chem.* 283:3618–3627.
32. George, T.C., S.L. Fanning, P. Fitzgeral-Bocarsly, R.B. Medeiros, S. Highfill, Y. Shimizu, B.E. Hall, K. Frost, D. Basiji, W.E. Ortyn, et al.

2006. Quantitative measurement of nuclear translocation events using similarity analysis of multispectral cellular images obtained in flow. *J. Immunol. Methods*. 311:117–129.
33. Li, L., Y. Iwamoto, A. Berezovskaya, and V.A. Boussiotis. 2006. A pathway regulated by cell cycle inhibitor p27Kip1 and checkpoint inhibitor Smad3 is involved in the induction of T cell tolerance. *Nat. Immunol.* 7:1157–1165.
34. Nolz, J.C., T.S. Gomez, P. Zhu, S. Li, R.B. Medeiros, Y. Shimizu, J.K. Burkhardt, B.D. Freedman, and D.D. Billadeau. 2006. The WAVE2 complex regulates actin cytoskeletal reorganization and CRAC-mediated calcium entry during T cell activation. *Curr. Biol.* 16:24–34.
35. Appleby, M.W., and F. Ramsdell. 2003. A forward-genetic approach for analysis of the immune system. *Nat. Rev. Immunol.* 3:463–471.
36. Cook, M.C., C.G. Vinuesa, and C.C. Goodnow. 2006. ENU-mutagenesis: insight into immune function and pathology. *Curr. Opin. Immunol.* 18:627–633.
37. Reynolds, L.F., C. de Bettignies, T. Norton, A. Beeser, J. Chernoff, and V.L. Tybulewicz. 2004. Vav1 transduces T cell receptor signals to the activation of the Ras/ERK pathway via LAT, Sos, and RasGRP1. *J. Biol. Chem.* 279:18239–18246.
38. Fujikawa, K., A.V. Miletic, F.W. Alt, R. Faccio, T. Brown, J. Hoog, J. Fredericks, S. Nishi, S. Mildiner, S.L. Moores, et al. 2003. Vav1/2/3-null mice define an essential role for Vav family proteins in lymphocyte development and activation but a differential requirement in MAPK signaling in T and B cells. *J. Exp. Med.* 198:1595–1608.
39. Costello, P.S., S.C. Cleverley, R. Galandrini, S.W. Henning, and D.A. Cantrell. 2000. The GTPase rho controls a p53-dependent survival checkpoint during thymopoiesis. *J. Exp. Med.* 192:77–85.
40. Henning, S.W., R. Galandrini, A. Hall, and D.A. Cantrell. 1997. The GTPase Rho has a critical regulatory role in thymus development. *EMBO J.* 16:2397–2407.
41. Tybulewicz, V.L. 2005. Vav-family proteins in T-cell signalling. *Curr. Opin. Immunol.* 17:267–274.
42. Gomez, T.S., S.D. McCarney, E. Carrizosa, C.M. Labno, E.O. Comiskey, J.C. Nolz, P. Zhu, B.D. Freedman, M.R. Clark, D.J. Rawlings, et al. 2006. HS1 functions as an essential actin-regulatory adaptor protein at the immune synapse. *Immunity*. 24:741–752.
43. Gomez, T.S., M.J. Hamann, S. McCarney, D.N. Savoy, C.M. Lubking, M.P. Heldebrant, C.M. Labno, D.J. McKean, M.A. McNiven, J.K. Burkhardt, and D.D. Billadeau. 2005. Dynamin 2 regulates T cell activation by controlling actin polymerization at the immunological synapse. *Nat. Immunol.* 6:261–270.
44. Zipfel, P.A., S.C. Bunnell, D.S. Witherow, J.J. Gu, E.M. Chislock, C. Ring, and A.M. Pendergast. 2006. Role for the Abi/wave protein complex in T cell receptor-mediated proliferation and cytoskeletal remodeling. *Curr. Biol.* 16:35–46.
45. Costello, P.S., A.E. Walters, P.J. Mee, M. Turner, L.F. Reynolds, A. Prisco, N. Sarner, R. Zamoyska, and V.L. Tybulewicz. 1999. The Rho-family GTP exchange factor Vav is a critical transducer of T cell receptor signals to the calcium, ERK, and NF-kappaB pathways. *Proc. Natl. Acad. Sci. USA*. 96:3035–3040.
46. Zhang, J., A. Shehabeldin, L.A. da Cruz, J. Butler, A.K. Somani, M. McGavin, I. Kozieradzki, A.O. dos Santos, A. Nagy, S. Grinstein, et al. 1999. Antigen receptor–induced activation and cytoskeletal rearrangement are impaired in Wiskott-Aldrich syndrome protein–deficient lymphocytes. *J. Exp. Med.* 190:1329–1342.
47. Tedford, K., L. Nitschke, I. Girkontaite, A. Charlesworth, G. Chan, V. Sakk, M. Barbacid, and K.D. Fischer. 2001. Compensation between Vav-1 and Vav-2 in B cell development and antigen receptor signaling. *Nat. Immunol.* 2:548–555.
48. Joshi, A.D., G.V. Hegde, J.D. Dickinson, A.K. Mittal, J.C. Lynch, J.D. Eudy, J.O. Armitage, P.J. Bierman, R.G. Bociek, M.P. Devetten, et al. 2007. ATM, CTLA4, MNDA, and HEM1 in high versus low CD38 expressing B-cell chronic lymphocytic leukemia. *Clin. Cancer Res.* 13:5295–5304.
49. Schwarzenberger, P., W. Huang, P. Ye, P. Oliver, M. Manuel, Z. Zhang, G. Bagby, S. Nelson, and J.K. Kolls. 2000. Requirement of endogenous stem cell factor and granulocyte-colony-stimulating factor for IL-17-mediated granulopoiesis. *J. Immunol.* 164:4783–4789.
50. Stark, M.A., Y. Huo, T.L. Burcin, M.A. Morris, T.S. Olson, and K. Ley. 2005. Phagocytosis of apoptotic neutrophils regulates granulopoiesis via IL-23 and IL-17. *Immunity*. 22:285–294.
51. Gakidis, M.A., X. Cullere, T. Olson, J.L. Wilsbacher, B. Zhang, S.L. Moores, K. Ley, W. Swat, T. Mayadas, and J.S. Brugge. 2004. Vav GEFs are required for $\beta_2$ integrin-dependent functions of neutrophils. *J. Cell Biol.* 166:273–282.
52. Li, S., A. Yamauchi, C.C. Marchal, J.K. Molitoris, L.A. Quilliam, and M.C. Dinauer. 2002. Chemoattractant-stimulated Rac activation in wild-type and Rac2-deficient murine neutrophils: preferential activation of Rac2 and Rac2 gene dosage effect on neutrophil functions. *J. Immunol.* 169:5043–5051.
53. Jansen, M., F.C. Yang, J.A. Cancelas, J.R. Bailey, and D.A. Williams. 2005. Rac2-deficient hematopoietic stem cells show defective interaction with the hematopoietic microenvironment and long-term engraftment failure. *Stem Cells*. 23:335–346.
54. Hummel, T., K. Leifker, and C. Klambt. 2000. The Drosophila HEM-2/NAP1 homolog KETTE controls axonal pathfinding and cytoskeletal organization. *Genes Dev.* 14:863–873.
55. Weiner, O.D., W.A. Marganski, L.F. Wu, S.J. Altschuler, and M.W. Kirschner. 2007. An actin-based wave generator organizes cell motility. *PLoS Biol.* 5:e221.
56. Justice, M.J., D.A. Carpenter, J. Favor, A. Neuhauser-Klaus, M. Hrabe de Angelis, D. Soewarto, A. Moser, S. Cordes, D. Miller, V. Chapman, et al. 2000. Effects of ENU dosage on mouse strains. *Mamm. Genome*. 11:484–488.
57. Kruszyna, R., R.P. Smith, and L. Ou. 1977. Method for measuring increased plasma hemoglobin in the presence of erythrocytes. *Clin. Chem.* 23:2156–2159.
58. Veldhoen, M., R.J. Hocking, C.J. Atkins, R.M. Locksley, and B. Stockinger. 2006. TGFbeta in the context of an inflammatory cytokine milieu supports de novo differentiation of IL-17-producing T cells. *Immunity*. 24:179–189.
59. Habib, T., H. Park, M. Tsang, I.M. de Alboran, A. Nicks, L. Wilson, P.S. Knoepfler, S. Andrews, D.J. Rawlings, R.N. Eisenman, and B.M. Iritani. 2007. Myc stimulates B lymphocyte differentiation and amplifies calcium signaling. *J. Cell Biol.* 179:717–731.
60. Iritani, B.M., K.A. Forbush, M.A. Farrar, and R.M. Perlmutter. 1997. Control of B cell development by Ras-mediated activation of Raf. *EMBO J.* 16:7019–7031.
61. Varnum-Finney, B., L.E. Purton, M. Yu, C. Brashem-Stein, D. Flowers, S. Staats, K.A. Moore, I. Le Roux, R. Mann, G. Gray, et al. 1998. The Notch ligand, Jagged-1, influences the development of primitive hematopoietic precursor cells. *Blood*. 91:4084–4091.